

REGULAR HYBRID WAVELETS AND DIRECTIONAL FILTER BANKS: EXTENSIONS AND APPLICATIONS

Ramin Eslami and Hayder Radha

e-mail: reslami@ieee.org and radha@egr.msu.edu

ECE Department, Michigan State University, East Lansing, MI 48824, USA

ABSTRACT

In a previous work, we proposed a new family of nonredundant geometrical image transforms using *Hybrid Wavelets and Directional filter banks* (HWD). In this paper we further develop and examine the proposed family and provide an efficient realization utilizing regular filters. Furthermore, we extend and employ the new proposed HWD transforms in two key image processing applications, coding and denoising, and demonstrate their promising results. For coding, an SPIHT-like algorithm is developed for HWD; and for denoising, a *translation-invariant HWD* (TIHWD) transform is constructed. Our simulations illustrate significant improvements under the proposed transforms when compared with other transform variations.

Index Terms— wavelet transforms, directional filter banks

1. INTRODUCTION

To construct an efficient image transform, the following criteria are critical. First, the transform should provide a good *nonlinear approximation* (NLA) [8] behavior. This requires the transform to be direction-sensitive (or geometric) in addition to being able to provide perfect reconstruction, multiresolution representation, and local support and analysis. Another important and related feature is the transform performance in terms of introducing a minimum level of ringing artifacts during NLA. The second criterion is that the transform should incur reasonable computational complexity. In the light of this property, fixed-procedure transforms are more desirable in contrast to adaptive transforms, which normally impose more computations. Finally, being nonredundant is a requirement in some image processing tasks such as image coding.

In [6] we introduced a new family of image transforms that satisfy the aforementioned criteria. In the present work we further develop and study their properties and show their applications to coding and denoising of natural images. This family is one of the first nonadaptive directional approaches that is employed for image coding. The proposed transform family is constructed using *Hybrid Wavelets and Directional filter banks* (HWD); thus we refer to them as the HWD transforms. We also extend this transform for the quincunx wavelets taking advantage of DFBs and provide NLA results.

A primary difference between our proposed transform family and other nonredundant transforms is the following. While HWD is nonadaptive, it possesses a rich set of directions, and provides an efficient NLA by taking advantage of the wavelet transform in its construction, and thus, it could be directly employed in key image processing applications such as embedded coding.

2. REGULAR HWD TRANSFORMS

To add directionality to the *wavelet transform* (WT), in a previous

work [7], we applied *directional filter banks* (DFB) [2] to all the highpass channels of WT, which resulted in introducing many artifacts in the smooth regions during NLA and coding. In this work, we address the problem based on the following conjuncture: When applying the DFB to the WT highpass channels, the primary source of ringing artifacts is due to employing the DFB to the coarser wavelet subbands.

The reasons justifying this conjuncture are as follows:

1) The human visual system is more sensitive to the low-frequency regions of images. Consequently, the ringing artifacts resulting from the coarser wavelet scales due to applying DFBs render more irritant distortions. In addition, smooth regions have transform coefficients mainly in the coarser scales of WT and are best represented by wavelet basis functions. Therefore, it is crucial to retain coarser wavelet subbands and do not change their basis elements.

2) Although the frequency scrambling that results from downsampling exists at all the levels of wavelet highpass channels, it is worse for coarser levels due to the lower frequency content of these subbands.

3) Suppose that a line segment of support size $\ell \times 1$ exists in the input image and we apply a J -level WT (we assign level one to the finest resolution). Then the support size of the line at a level j ($1 \leq j \leq J$) is approximately $[(1-2^{-j})\ell_g + 2^{-j}\ell] \times (1-2^{-j})\ell_g$ for the diagonal subband (a similar expression can be obtained for other subbands), where ℓ_g is the length of the highpass filter $g^{(ld)}[n]$. Observe that the line segment becomes thicker in coarser scales; as a result, it is not a suitable line segment for the DFB.

4) Since large-size fan filters are employed in the DFB, the size of coarser subbands usually becomes less than the size of the DFB filters applied to them. In this case, we take advantage of the periodic extension of the signal. It turns out that a distorted version of the input signal $x[n]$ is employed in filtering [4], which makes the output distorted. \square

By applying DFBs to a few finest scales of the WT, we convert some of the wavelet basis functions to *directional* elements representing edges in an image while we keep *nondirectional* basis functions in the coarser wavelet scales to best represent smooth regions. Since in the WT we already have horizontal and vertical subbands, different paradigms could be considered to apply DFBs to the $J_m < J$ finest subbands of wavelets. As a result, we propose three types of HWD transforms:

• HWD Type 1:

- i. Apply *Vertical DFBs* (VDFBs) [6] with l_j levels to *vertical* wavelet subbands at levels $1 \leq j \leq J_m$. We denote these subbands by $\text{VD}_j^{(i)}$ ($i \in I_v^{(l_j)} = \{i \mid i = 'h' \text{ or } 2^{l_j-1} < i \leq 2^{l_j}\}$).
- ii. Apply *Horizontal DFBs* (HDFBs) [6] with l_j levels to *horizontal* wavelet subbands at levels $1 \leq j \leq J_m$. We denote these subbands by $\text{HD}_j^{(i)}$ ($i \in I_h^{(l_j)} = \{i \mid 1 \leq i \leq 2^{l_j-1} \text{ or } i = 'v'\}$).

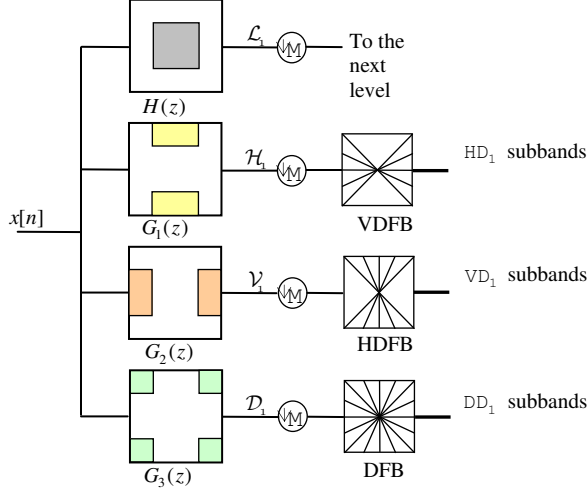


Fig. 1. The HWD2 transform using $l_1 = 3$ directional levels.

iii. Apply (full-tree) *DFBs* with l_j levels to *diagonal* wavelet subbands at levels $1 \leq j \leq J_m$. We denote these subbands by $DD_j^{(i)}$ ($i \in I_d^{(l_j)} = \{i \mid 1 \leq i \leq 2^{l_j}\}$).

• **HWD Type 2:**

i. Apply *HDFBs* with l_j levels to *vertical* wavelet subbands at levels $1 \leq j \leq J_m$. We denote these subbands by $VD_j^{(i)}$ ($i \in I_v^{(l_j)}$)

ii. Apply *VDFBs* with l_j levels to *horizontal* wavelet subbands at levels $1 \leq j \leq J_m$. We denote these subbands by $HD_j^{(i)}$ ($i \in I_h^{(l_j)}$)

iii. Apply (full-tree) *DFBs* with l_j levels to *diagonal* wavelet subbands at levels $1 \leq j \leq J_m$. We denote these subbands by $DD_j^{(i)}$ ($i \in I_d^{(l_j)}$)

• **HWD Type 3:**

Apply (full-tree) *DFBs* with l_j levels to all three highpass subbands of wavelets at levels $1 \leq j \leq J_m$. We denote the subbands by $VD_j^{(i)}$, $HD_j^{(i)}$, and $DD_j^{(i)}$ ($i \in I_d^{(l_j)}$) corresponding to the *vertical*, *horizontal*, and *diagonal* wavelet subbands to which we applied the *DFBs*.

In summary, we extend the directionality of the original finest wavelet subbands. In type 2 we can avoid frequency scrambling due to the downsampling of wavelet subbands to some extent [4]. In type 3 we use a maximum level of directional extension. A schematic diagram of the HWD type 2 (or HWD2) is illustrated in Fig. 1.

Using the noble identities, we can move the *DFB* filters before downsampling by $M = \text{diag}(2, 2)$ in the WT. Consequently, we can find the frequency partitioning by the HWD family as Fig. 2 demonstrates. Note that in HWD1 and 3, since some of the *DFB* filters are oriented similar to the wavelet subbands, the level of artifacts during NLA is higher, while they better retrieve directional features in the image when compared with HWD2.

Similar to the HWD, we can add directionality to the *quincunx wavelet transform* (QWT) to construct *Hybrid Quincunx Wavelets and Directional filter banks* (HQWD). In contrast to the WT, the QWT uses nonseparable diamond filters and has just one highpass channel. As a result, we propose the HQWD transform as follows (see Fig. 3(a)):

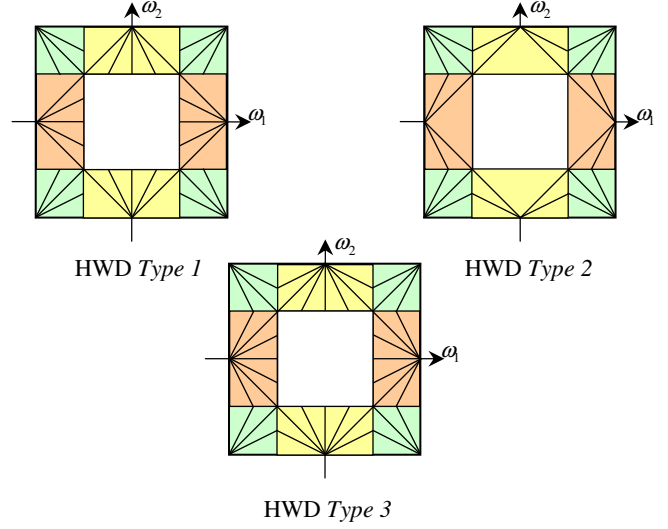


Fig. 2. The frequency partitioning in the HWD family using $l_1 = 3$ directional levels.

• **HQWD:**

Apply (full-tree) *DFBs* with l_j levels to the highpass subbands of quincunx wavelets at levels $1 \leq j \leq J_m$. We denote the resulting subbands by $QD_j^{(i)}$ ($1 \leq i \leq 2^{l_j}$).

Again, after using noble identities, the frequency span of the HQWD is obtained as Fig. 3(b) shows. A few basis functions are depicted in Fig. 3(c).

In the HWD, the number of directions in the *DFB* stage (l_j) and the number of finest wavelet scales (J_m) are dependent on the image size and the amount of textures in the image. For texture images and images with a significant amount of texture regions we use larger values of the directional levels. To address item 4 (above) of our conjuncture, for a given image of size $N \times N$ and fan filter pair of the *DFB* with maximum support size of (ℓ_f, ℓ_f) , we should have $J_m < \log_2 N / 2\ell_f$, where l_{J_m} is assumed to be 2 (the minimum number of directional levels). Note that for the HQWD we have $J_m < 2 \log_2(N / 2\ell_f)$.

Now we provide an efficient realization for the proposed transform family. Regularity of the filters in the HWD family is of

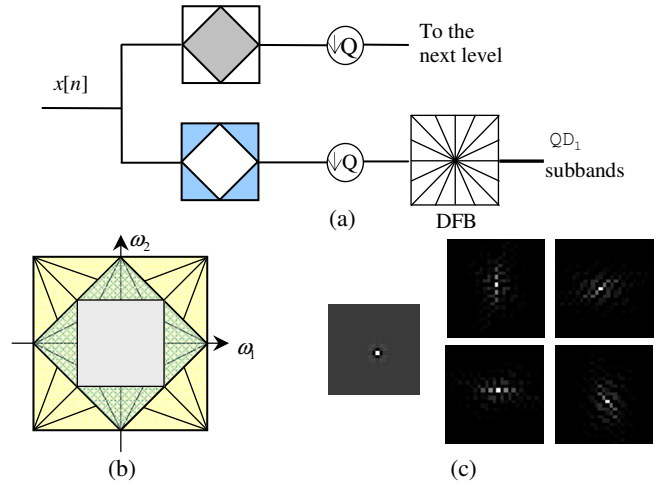


Fig. 3. (a) The HQWD transform (white areas in QFB show stopbands). (b) The frequency partitioning in the HQWD $l_1 = l_2 = 3$ directional levels. (c) *Left*: A basis function of the QWT. *Right*: Some directional basis functions of the HQWD.

key importance. Having regular filters in a transform, we obtain NLA results possessing less visible artifacts. This is more crucial in the case of HWD where we have to use DFB filters with large support to achieve better directional resolution.

Another important factor is computational complexity. We wish to do nonseparable filtering with a complexity comparable to the separable one. A solution to this is employing ladder networks that perform nonseparable filtering in the polyphase domain using separable filters as proposed in [9]. The procedure based on double-halfband filter bank [9], however, has some restrictions. Ansari *et al.* addressed the issue by introducing triplet-based filter banks [1]. In this scheme, we can choose the kernel function as Lagrange polynomials, which provide maximally-flat halfband filters. Therefore, we construct regular fan filters using transformation $R(z) = R^{(ld)}(-z_1)R^{(ld)}(-z_2)$, where $R^{(ld)}(z)$ is the 1-D kernel function [4]. For the WT stage of the HWD, we use Daubechies 9/7 filters.

Using linear-phase filters in the HWD, the resulting complexities for the analysis banks are about

$$(4/3)\ell_h + 3(3N_T + 1) \sum_{j=1}^{J_m} (\ell_j/4^j) \quad \text{MPS,}$$

and

$$(4/3)\ell_h + 9(N_T - 1/2) \sum_{j=1}^{J_m} (\ell_j/4^j) \quad \text{APS,}$$

for HWD3, and

$$(4/3)\ell_h + (3N_T + 1) \sum_{j=1}^{J_m} ((2l_j + 1)/4^j) \quad \text{MPS,}$$

and

$$(4/3)\ell_h + 3(N_T - 1/2) \sum_{j=1}^{J_m} ((2l_j + 1)/4^j) \quad \text{APS,}$$

for HWD1 and 2 transforms. Here $N_T = \ell_r/2$, where ℓ_r is the length of $R^{(ld)}(z)$; ℓ_h is the length of 1-D wavelet filter (we assumed same lowpass and highpass filter size); MPS and APS denote *multiplications per input samples* and *additions per input samples*.

3. APPLICATIONS

3.1. Nonlinear Approximation

Nonlinear approximation (NLA) is an efficient approach to measure the capability of a transform in sparse representation of a signal.

We tested our proposed transforms using a variety of images and compared them with other transforms such as WT and contourlets [3]. In all experiments we employed the following settings. We used five decomposition levels in all of the methods and Daubechies 9/7 filters for the WT. For the HWD transforms we set $J_m = 2$. For contourlets we used $\{l_j\}_{\leq 1 \leq j \leq 5} = \{5, 4, 4, 3, 3\}$ directional levels. For the *Barbara* image we used HWD3 with $l_1 = l_2 = 3$ directional levels while for other images we used HWD2 with $l_1 = l_2 = 2$.

Some numerical values for the NLA of the *Barbara* image are given in Table I. To demonstrate the effect of employing regular fan filters in the HWD, we also provided the HWD results when using double-halfband filters. The fan filter pair have support size of (23, 23) and (45, 45) in double- and support size of (29, 29) and (43, 43) in triple-halfband ladder structures.

The proposed HWD transform shows promising results for the *Barbara* image (and other images with significant texture content) where it consistently outperforms both wavelets and contourlets. In particular, it achieves up to 1.6 dB (1.2 dB) improvement over the WT (contourlet transform).

We also performed NLA for the HQWD transform and compared it with the quincunx wavelet transform. Table II shows the PSNR values obtained for the *Barbara* image. As seen, HQWD provides a growing improvement in the PSNR values as the number of retained coefficients increases. In this experiment we

TABLE I
PSNR VALUES OF THE NLA EXPERIMENT FOR THE *BARBARA* IMAGE

Method / M	2048	4096	8192	16374	32768
HWD (THF) ¹	23.91	25.86	28.28	31.35	35.39
HWD (DHF) ²	23.87	25.73	28.05	30.95	34.73
Wavelets	23.33	24.63	26.68	29.95	34.58
Contourlets [3]	23.29	24.95	27.08	29.63	32.91

M denotes the number retained significant coefficients.

¹HWD using triple-halfband filters for the DFB.

²HWD using double-halfband filters for the DFB.

TABLE II
PSNR VALUES OF THE NLA EXPERIMENT FOR THE *BARBARA* IMAGE

Method / M	2048	4096	8192	16374	32768
HQWD	22.21	23.69	25.59	28.18	31.90
Quincunx WT	21.95	23.06	24.54	26.64	30.06

used ten wavelet levels and for the HQWD we used $J_m = 4$ and $l_j = 3$ ($1 \leq j \leq J_m$).

3.2. Image Coding

Regarding the good NLA performance of the HWD family and since this transform family is nonredundant, a potential key application for the proposed transforms is image coding.

Although the NLA decay rate of wavelets for images is suboptimal, one can benefit from tree-based coding schemes such as the SPIHT algorithm [10] to improve this decay rate. In this scheme, inter-scale dependencies are exploited through the parent-children relationships existing among the wavelet coefficients.

To take advantage of the SPIHT scanning algorithm for the HWD transform coefficients, a new parent-children relationship should be considered. Suppose that we have an HWD transform with J levels. For the levels $J_m < j \leq J$, we have the same relationship as the one in the WT, and for the levels $1 \leq j \leq J_m$, for each subband HD_j , VD_j , and DD_j we can use a similar parent-children relationship as the one considered for the contourlet coefficients [11]. The problem appears when we attempt to define children of coefficients lying at level $J_m + 1$. By applying DFBs to level J_m , we almost remove the inter-scale dependencies that existed between wavelet levels J_m and $J_m + 1$. Nevertheless, we employ a suboptimal but simple rearrangement algorithm to be able to apply a similar SPIHT scanning algorithm as the one we use for wavelets [4].

Fig. 4 shows coding results of the *Barbara* image at 0.25 bpp. As seen, more directional features are retained when using the HWD transform. Further, we have improved PSNR values compared with those of the wavelet coder. Note that in these results, the rates are calculated from the entropy of the output bitstreams.

3.3. Image Denoising

Image denoising is another application of the HWD transforms. We tested the proposed transforms for denoising of noisy images corrupted with additive Gaussian noise. We used a simple hard-thresholding rule to shrink the transform coefficients. The threshold is selected as 3σ [8] where σ is the standard deviation of the input noise and is estimated using robust median estimator. We also mirror-extended the images to remedy boundary artifacts.

Since the HWD transforms are shift variant, they introduce many artifacts in the denoising results. Therefore, we also constructed *translation-invariant HWD* (TIHWD) transforms by removing subsampling operations to improve the results. A delicate point in developing the TIHWD schemes, is that we should not change the frequency partitioning of the HWD



Wavelets/SPIHT; PSNR = 27.45 HWD3/SPIHT; PSNR = 27.83

Fig. 4. Coding result of the *Barbara* image at rate 0.25 bpp.

transforms (see Fig. 2). As a result, we first upsample the DFB filters at level j ($1 \leq j \leq J_m$) by M^j , where $M = \text{diag}(2, 2)$ and then remove the sampling operations using the *generalized algorithm à trous* introduced in [5].

In addition to the proposed methods, we also employed the *wavelet transform* (WT), *contourlet transform* (CT) [3], and *translation-invariant WT* (TIWT). Table III shows the PSNR values of the denoising results for two images and different noise levels. As seen, the HWD transform yields in better PSNR values than the CT. Moreover, for the *Barbara* image it achieves superior results when compared with the WT. In the case of *translation-invariant* (TI) denoising, we see that the proposed TIHWD denoising scheme always provides better results (improvements up to 1.80 dB) when compared with the TIWT scheme.

Fig. 5 shows some visual results of the TI denoising. We see that the TIHWD scheme provides less visible artifacts in the denoised images while it has superior performance in retaining details.

4. CONCLUSION

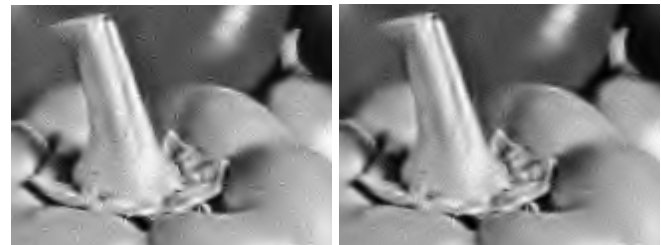
The new family of HWD transforms benefit from both directional and nondirectional basis functions providing promising NLA performance. In this paper, we further studied and developed the proposed transforms and employed them in image coding and denoising applications and demonstrated their potential in these areas.

5. REFERENCES

- [1] R. Ansari, C. W. Kim, and M. Dedovic, "Structure and design of two-channel filter banks derive from a triplet of halfband filters," *IEEE Trans. CAS-II*, vol. 46, pp. 1487-1496, Dec. 1999.
- [2] R. H. Bamberger and M. J. T. Smith, "A filter bank for the directional decomposition of images: Theory and design," *IEEE Trans. Signal Processing*, vol. 40, no. 4, pp. 882-893, Apr. 1992.
- [3] M. N. Do and M. Vetterli, "The contourlet transform: An efficient directional multiresolution image representation," *IEEE Trans. Image Processing*, vol. 14, no. 12, pp. 2091-2106, Dec. 2005. Software available on <http://www.ifp.uiuc.edu/~minhdo/software/>.
- [4] R. Eslami and H. Radha, "A new family of nonredundant transforms using hybrid wavelets and directional filter banks," *IEEE Trans. Image Processing*, 2006.

TABLE III
PSNR VALUES OF THE DENOISING EXPERIMENTS

Image	σ	Noisy Image	WT	CT [3]	HWD	TIWT	TIHWD
<i>Barbara</i>	10	28.13	29.86	29.78	30.07	32.58	33.70
	20	22.15	25.80	26.31	26.58	28.26	30.01
	40	16.38	22.44	22.94	23.16	24.53	26.33
	60	13.30	20.99	21.04	21.21	22.82	23.96
<i>Peppers</i>	10	28.25	31.83	31.04	31.69	33.91	33.95
	20	22.32	28.49	27.89	28.43	30.97	31.18
	40	16.59	24.47	24.09	24.46	27.06	27.44
	60	13.53	22.00	21.64	21.91	24.38	24.71



TIWT; PSNR = 30.97

TIHWD; PSNR = 31.18



TIWT; PSNR = 24.53



TIHWD; PSNR = 26.33

Fig. 5. Denoising results of the *Peppers* image when $\sigma = 20$ and the *Barbara* image when $\sigma = 40$.

- [5] R. Eslami and H. Radha, "Image denoising using translation-invariant contourlet transform," *IEEE Int. Conf. Acoustics, Speech, and Signal Processing*, vol. 4, pp. 557-560, Mar. 2005.
- [6] R. Eslami and H. Radha, "New image transforms using hybrid wavelets and directional filter banks: analysis and design," *IEEE Int. Conf. Image Processing*, vol. 1, pp. 733-736, Sep. 2005.
- [7] R. Eslami and H. Radha, "Wavelet-based contourlet transform and its application to image coding," *IEEE Int. Conf. Image Processing*, vol. 5, pp. 3189-3192, Oct. 2004.
- [8] S. Mallat, *A Wavelet Tour of Signal Processing*. Academic Press, 2nd Ed., 1998.
- [9] S. Phoong, C. Kim, P. Vaidyanathan, and R. Ansari, "A new class of two-channel biorthogonal filter banks and wavelet bases," *IEEE Trans. Signal Processing*, vol. 43, pp. 649-665, Mar. 1995.
- [10] A. Said and W. A. Pearlman, "A new fast and efficient image codec based on set partitioning in hierarchical trees," *IEEE Trans. Circuits and Systems for Video Technology*, vol. 6, pp. 243-250, Jun. 1996.
- [11] D. D.-Y. Po and M. N. Do, "Directional multiscale modeling of images using the contourlet transform," *IEEE Trans. Image Processing*, vol. 15, pp. 1610-1620, Jun. 2006.